Video Article

In-depth Physiological Analysis of Defined Cell Populations in Acute Tissue Slices of the Mouse Vomeronasal Organ

Tobias Ackels[1,2], Daniela R. Drose[1], Marc Spehr[1]

[1]Department of Chemosensation, Institute for Biology II, RWTH Aachen University

[2]Mill Hill Laboratory, The Francis Crick Institute

Correspondence to: Tobias Ackels at tobias.ackels@crick.ac.uk

URL: http://www.jove.com/video/54517
DOI: doi:10.3791/54517

Keywords: Neuroscience, Issue 115, Vomeronasal organ, olfaction, acute slice preparation, patch-clamp, electrophysiology, sensory neurons, formyl peptide receptor

Date Published: 9/10/2016

Citation: Ackels, T., Drose, D.R., Spehr, M. In-depth Physiological Analysis of Defined Cell Populations in Acute Tissue Slices of the Mouse Vomeronasal Organ. *J. Vis. Exp.* (115), e54517, doi:10.3791/54517 (2016).

Abstract

In most mammals, the vomeronasal organ (VNO) is a chemosensory structure that detects both hetero- and conspecific social cues. Vomeronasal sensory neurons (VSNs) express a specific type of G protein-coupled receptor (GPCR) from at least three different chemoreceptor gene families allowing sensitive and specific detection of chemosensory cues. These families comprise the *V1r* and *V2r* gene families as well as the formyl peptide receptor (FPR)-related sequence (*Fpr-rs*) family of putative chemoreceptor genes. In order to understand the physiology of vomeronasal receptor-ligand interactions and downstream signaling, it is essential to identify the biophysical properties inherent to each specific class of VSNs.

The physiological approach described here allows identification and in-depth analysis of a defined population of sensory neurons using a transgenic mouse line (Fpr-rs3-i-Venus). The use of this protocol, however, is not restricted to this specific line and thus can easily be extended to other genetically modified lines or wild type animals.

Video Link

The video component of this article can be found at http://www.jove.com/video/54517/

Introduction

Most animals rely heavily on their chemical senses to interact with their surroundings. The sense of smell plays an essential role for finding and evaluating food, avoiding predators and locating suitable mating partners. In most mammals, the olfactory system consists of at least four anatomically and functionally distinct peripheral subsystems: the main olfactory epithelium[1,2], the Grueneberg ganglion[3,4], the septal organ of Masera[5,6] and the vomeronasal organ. The VNO comprises the peripheral sensory structure of the accessory olfactory system (AOS), which plays a major role in detecting chemical cues that convey information about identity, gender, social rank and sexual state[7-10]. The VNO is located at the base of the nasal septum right above the palate. In mice, it is a bilateral blind-ending tube enclosed in a cartilaginous capsule[11-13]. The organ consists of both a crescent-shaped medial sensory epithelium that harbors the VSNs and of a non-sensory part on the lateral side. Between both epithelia lies a mucus-filled lumen which is connected to the nasal cavity via the narrow vomeronasal duct[14]. A large lateral blood vessel in the non-sensory tissue provides a vascular pumping mechanism to facilitate entry of relatively large, mostly non-volatile molecules such as peptides or small proteins into the VNO lumen through negative pressure[15,16]. The structural components of the VNO are present at birth and the organ reaches adult size shortly before puberty[17]. However, whether the rodent AOS is already functional in juveniles is still subject to debate[18-20].

VSNs are distinguished by both their epithelial location and the type of receptor they express. VSNs show a bipolar morphology with an unmyelinated axon and a single apical dendrite that protrudes towards the lumen and ends in a microvillous dendritic knob. VSN axons fasciculate to form the vomeronasal nerve that leaves the cartilaginous capsule at the dorso-caudal end, ascends along the septum, passes the cribriform plate and projects to the accessory olfactory bulb (AOB)[21,22]. The vomeronasal sensory epithelium consists of two layers: the apical layer is located closer to the luminal side and harbors both V1R- and all but one type of FPR-rs-expressing neurons. These neurons coexpress the G-protein α-subunit $G_{\alpha i2}$ and project to the anterior part of the AOB[23-25]. Sensory neurons located in the more basal layer express V2Rs or FPR-rs1 alongside $G_{\alpha o}$ and send their axons to the posterior region of the AOB[26-28].

Vomeronasal neurons are likely activated by rather small semiochemicals[29-33] (V1Rs) or proteinaceous compounds[34-38] (V2Rs) that are secreted into various bodily fluids such as urine, saliva and tear fluid[37,39-41]. *In situ* experiments have shown that VSNs are also activated by formylated peptides and various antimicrobial/inflammation-linked compounds[25,42]. Moreover, heterologously expressed FPR-rs proteins share agonist spectra with FPRs expressed in the immune system, indicating a potential role as detectors for sickness in conspecifics or spoiled food sources[25] (see reference[43]).

Fundamental to understanding receptor-ligand relationships and downstream signaling cascades in specific VSN populations is a detailed evaluation of their basic biophysical characteristics in a native environment. In the past, the analysis of cellular signaling has greatly benefitted from genetically modified animals that mark a defined population of neurons by coexpressing a fluorescent marker protein[30,44-49]. In this protocol, a transgenic mouse line that expresses FPR-rs3 together with a fluorescent marker (Fpr-rs3-i-Venus) is used. This approach exemplifies how to employ such a genetically modified mouse strain to perform electrophysiological analysis of an optically identifiable cell population using single neuron patch-clamp recordings in acute coronal VNO tissue slices. An air pressure-driven multi-barrel perfusion system for sensory stimuli and pharmacological agents allows quick, reversible and focal neuronal stimulation or inhibition during recordings. Whole-cell recordings in slice preparations allow for a detailed analysis of intrinsic properties, voltage-activated conductances, as well as action potential discharge patterns in the cell's native environment.

Protocol

All animal procedures were in compliance with local and European Union legislation on the protection of animals used for experimental purposes (Directive 86/609/EEC) and with recommendations put forward by the Federation of European Laboratory Animal Science Associations (FELASA). Both C57BL/6 mice and Fpr-rs3-i-Venus mice were housed in groups of both sexes at room temperature on a 12 hr light/dark cycle with food and water available *ad libitum*. For experiments young adults (6-20 weeks) of either sex were used. No obvious gender-dependent differences were observed.

1. Solution Preparation

1. Prepare extracellular solution S_1: 4-(2-Hydroxy-ethyl)piperazine-1-ethanesulfonic acid (HEPES) buffered extracellular solution containing (in mM) 145 NaCl, 5 KCl, 1 $CaCl_2$, 1 $MgCl_2$, 10 HEPES; pH = 7.3 (adjusted with NaOH); osmolarity = 300 mOsm (adjusted with glucose).
2. Prepare extracellular solution S_2: Carbogen-oxygenated (95% O_2, 5% CO_2) extracellular solution containing (in mM) 125 NaCl, 25 $NaHCO_3$, 5 KCl, 1 $CaCl_2$, 1 $MgSO_4$, 5 BES; pH = 7.3; osmolarity = 300 mOsm (adjusted with glucose).
3. Prepare 4% low-gelling temperature agarose solution (S_3) for tissue embedding: 4% low-gelling temperature agarose. Dissolve 2 g low-gelling agarose in 50 ml of S_1 in a 100 ml glass laboratory bottle together with a magnetic stirrer. To melt the agarose, put the bottle in a water bath (with lid not tightly closed) at 70 °C for approximately 20 min or until solution becomes transparent while stirring. Cool down and keep melted agarose in a second water bath at 42 °C until further use.
4. Prepare intracellular solution S_4: Pipette solution containing (in mM) 143 KCl, 2 KOH, 1 EGTA, 0.3 $CaCl_2$ (free Ca^{2+} = 110 nM), 10 HEPES, 2 MgATP, 1 NaGTP; pH = 7.1 (adjusted with KOH); osmolarity = 290 mOsm.
5. Modify/adjust composition of S_1, S_2 and S_4 according to individual experimental design (*e.g.*, pharmacological blockers to isolate certain types of voltage-activated currents).

2. Workspace Preparation

1. Fill oxygenating slice storing chamber with S_2 at least 30 min prior to dissection, place on ice for temperature and pH adjustment and oxygenate solution continuously.
2. Fill reservoir for slice superfusion at recording setup with S_2 and oxygenate continuously.
3. Prior to dissection, fill vibratome chamber with S_2 and arrange crushed ice around the chamber. Alternatively, transfer spare ice cold oxygenated solution from oxygenating chamber into vibratome chamber and keep oxygenating continuously.
4. Arrange surgical tools and consumables.
5. Place ice gel pack under dissecting microscope, cover with a paper towel to prevent VNO tissue from freezing to bottom of the dish.
6. Clean razor blade by briefly rinsing in 70% ethanol and distilled water and mount to vibratome. Replace for every slicing session.

3. VNO Dissection and Embedding

1. Sacrifice animal by brief exposure to CO_2 and decapitate using sharp surgical scissors. Note: As time from sacrificing the animal to putting the VNO capsule on ice is critical, minimize the time to less than 2 min. To maintain tissue viability, embed both fully dissected VNOs in agarose in less than 30 min.
2. Remove the lower jaw with large surgical scissors. Enter through the mouth cavity and cut the mandible bones and muscle of each side separately.
3. Place the remaining part of the head upside down in the large Petri dish.
4. Pull away the skin of the upper jaw and around the tip of the nose with medium forceps to gain better access to the incisors.
5. Use bone scissors to cut away the largest part of the incisors at a ~45° angle in the rostral direction (**Figure 1A**). This will ease removal of the VNO capsule from the nasal cavity.
   Note: Do not cut to the root of the tooth to prevent damage to the tip of the VNO capsule.
6. Grab the rigid upper palate at its rostral part with medium forceps and carefully peel back in one piece at a flat angle (**Figure 1B**).
   Note: Repeatedly rinse with ice-cold S_2.
7. Use micro spring scissors to cut the bony fusion between the tip of the vomer bone and the jaw. Insert the scissor tips with the curved part of the tip pointing outward away from the VNO and carefully cut the bone in small steps on both the left and right side lateral to the VNO capsule.
8. To remove the VNO capsule, use micro spring scissors to cut through the vomer bone at the caudal part and carefully lift the vomer bone out of the nasal cavity using medium forceps. Immediately transfer the VNO to a small petri dish under a stereo microscope on an ice gel pack where the remaining steps of the dissection will be performed.
9. Rinse the VNO in a small amount of ice-cold S_2 to prevent the tissue from drying out.
10. Separate the cartilaginous capsules that contain the VNO soft tissues by grabbing the back of the vomer bone with medium forceps. Position the capsule for a dorsal view so that a split between both VNOs becomes visible (**Figure 1D$_i$**).

11. Use the tip of fine forceps to separate both cartilage VNO capsules from the central bone while keeping the vomer bone pinned down at the rear part.
    Note: Use forceps only at the rim of the cartilage capsule and be very careful not to pierce through the cartilage as the delicate sensory epithelium is easily damaged.
12. Once the two VNOs are separated, start removing the cartilage encapsulating the first VNO.
13. Grab the top rim of the capsule with one fine forceps and split away the cartilage wall that was previously attached to the vomer bone (medial side).
14. To remove remaining cartilage turn the VNO with its curved lateral side to the bottom of the dish and securely pin down the cartilage on one side using forceps. Carefully move the second fine forceps from the back side at a very flat angle between cartilage and VNO to loosen the connection between tissue and cartilage.
15. Slowly peel the VNO away from the cartilage by holding it at its caudal tip, to avoid damaging the sensory epithelium.
16. Once the VNO is levered from the capsule, make sure to remove all remaining small cartilage parts as any remaining pieces of cartilage will detach the tissue from surrounding agarose during the slicing process.
17. Place a small drop of ice-cold S_2 on the first dissected VNO to prevent tissue damage. A large blood vessel on the lateral side will become visible indicating that the organ is still intact and was not grossly damaged during the dissection (**Figure 2A$_{ii}$**). In case the blood vessel got damaged, it will still be worthwhile to carry on with slicing the VNO as long as the overall morphology was not clearly impaired.
18. Immediately dissect the second VNO.
19. To embed the VNOs, fill both small petri dishes to the rim with melted S_3 (stored in water bath at 42 °C; see 1.3).
20. Hold the VNO on the broader caudal end with fine forceps to avoid damage to the sensory epithelium.
21. Immerse the VNO in the agarose and move it horizontally back and forth several times to remove the film of extracellular solution as well as any air bubbles from its surface.
22. Position the VNO vertically with the caudal tip facing the bottom of the dish. Instead of pinching the VNO with the forceps directly, adjust orientation by moving the forceps tip in close proximity to the VNO.
    Note: Orientation during embedding is crucial as it determines slice plane and accessibility to sensory neurons during the experiment.
23. Place dishes on gel ice pack and wait until agarose has solidified.
    Note: Do not change VNO orientation once the agarose has started solidifying as this will detach the tissue from the surrounding agarose.

4. Coronal VNO Tissue Slicing

1. Use small spatula to remove agarose block from the small dish into the lid of a large Petri dish, flip the agarose upside down leaving the caudal tip of the VNO facing upwards.
2. Cut the block into a pyramidal shape using a surgical scalpel (3-4 mm at the tip, 8-10 mm at the bottom). Take care not to damage the embedded tissue.
3. Use super glue to fix the pyramid-shaped block to the center of the vibratome specimen plate and wait ~1 min for the glue to dry completely.
4. Transfer the specimen plate to the slicing chamber and prepare the second VNO, accordingly. Keep plate with the second specimen at 4 °C until use.
5. Use a vibrating blade microtome with the following settings: thickness: 150-200 µm; speed: 3.5 a.u. = 0.15 mm/sec; frequency: 7.5 a.u. = 75 Hz. Transfer slices to oxygenating chamber until use after briefly inspecting slice morphology under the dissecting microscope. Slices can be kept for several hr.

5. Single-cell Electrophysiological Recordings

1. For recordings, use an upright fixed-stage microscope equipped with water immersion objectives, Dodt or infrared differential interfering contrast (IR-DIC), and epi-fluorescence as well as a cooled CCD-camera. For data acquisition, use a patch-clamp amplifier, head stage, AD/DA interface board and a PC (including recording software).
2. Prepare a stock of 10-20 patch pipettes (4-7 MΩ). Pull pipettes from borosilicate glass capillaries (1.50 mm OD/0.86 mm ID) using a micropipette puller and fire-polish with a microforge.
   Note: Fire polishing the pipette tips is crucial when patching the rather small VSNs. This will help to prevent rupturing the cell membrane when applying negative pressure in order to obtain a high resistance seal. After polishing the pipette opening should be approximately 1 µm.
3. Keep pipettes in a pipette storage jar to prevent damage and dust accumulation until use.
4. Prepare perfusion system by filling solution reservoirs and tubing according to experimental design.
   Note: Remove air bubbles from tubing completely as they will strongly interfere with electrophysiological recordings.
5. Adjust pressure to achieve ~3 ml/min flow.
   Note: High pressures will cause movement of the tissue slice as well as termination of electrophysiological recordings.
6. Transfer VNO slice to imaging chamber and fix the slice position using stainless steel anchor wired with 0.1 mm thick synthetic fibers (**Figure 2B**-**C**).
   Note: Do not cover the tissue slice with one of the synthetic fiber threads but rather the agarose surrounding the slice.
7. Transfer imaging chamber to recording setup and continuously superfuse slice with oxygenated S_2 at room temperature via a bath application.
8. Adjust the suction capillary to the surface of the solution to create a slow suction for constant exchange of bath solution. Adjust the 8-in-1 multi-barrel "perfusion pencil" above and close to the non-sensory part of the VNO slice that contains the blood vessel (**Figure 2C**, **3A**)[50]. It will be beneficial to arrange perfusion pencil and recording pipette to be facing the slice from opposite directions.
9. Connect reference electrode and bath solution using an L-shaped agar bridge (filled with 150 mM KCl).
10. Fill patch pipette with pipette solution S_4.
11. Mount the pipette over the silver chloride-coated patch electrode connected to the head stage without scraping off the coating and attach firmly.
12. Apply slight positive pressure (approximately 1 ml on a 10 ml plastic syringe) to the patch pipette before entering the bath.
13. Lower the pipette into the bath using micro manipulators far enough to be able to submerge the objective without hitting it (**Figure 2D**).

14. Monitor pipette resistance (R_{pip}, between 4-7 MΩ) using electrophysiology software connected to the head stage.
    Note: If R_{pip} is <4 MΩ the glass tip is broken. If R_{pip} is >10 MΩ, the tip is most likely clogged and the pipette must be replaced.
15. Visualize the VNO slice with a CCD-camera using infrared-optimized differential interference contrast (DIC) and identify FPR-rs3-i-Venus expressing cells (or similarly labeled neurons) using fluorescence illumination and an appropriate filter cube.
16. Focus and target fluorescent or non-fluorescent cells depending on experimental design.
17. To approach the cell body, use hand wheels for maximum sensitivity. Due to positive pressure, a small dent in the cell soma membrane becomes visible once the pipette tip is in close proximity.
18. Release positive pressure and apply slight negative pressure to suck in the cell membrane in order to gain a high resistance seal (1-20 GΩ). Apply short and gentle suction to disrupt the cell membrane and establish the whole-cell configuration.
19. Monitor access resistance constantly during experiment.
    Note: Only include neurons exhibiting small and stable access resistance (≤3% of R_{input}; change <20% over the course of the experiment) into analysis.

Representative Results

To gain insight into the biophysical and physiological properties of defined cell populations, we perform acute coronal tissue slices of the mouse VNO (**Figure 1**-**2**). After dissection, slices can be kept in ice-cold oxygenated extracellular solution (S_2) for several hr. At the recording setup, a constant exchange with fresh oxygenated solution (**Figure 2D**) ensures tissue viability throughout the experiment. We here employ a transgenic mouse model (FPR-rs3-i-Venus). VSNs in this strain coexpress a fluorescent marker protein with FPR-rs3, a prototypical member of the *FPR-rs* gene family (**Figure 3**) enabling optical identification of a defined population of sensory neurons. Electrophysiological recordings provide the means for in-depth analysis at the single-cell level. For instance, analysis of voltage-gated currents is performed in the voltage-clamp mode (**Figure 4A**-**B**). To isolate specific types of ionic currents, slices are superfused with pharmacological agents such as TTX to inhibit voltage-gated Na^+ currents (**Figure 4A**) or nifedipine to block voltage-gated L-type Ca^{2+} currents (**Figure 4B**). Furthermore, we routinely perform whole-cell recordings in the current clamp configuration to analyze action potential discharge patterns (**Figure 4C**). In addition to whole-cell recordings, cell-attached 'loose-seal' recordings provide a less invasive method that prevents dialysis of intracellular components **(Figure 5A)**. Recording action potential-driven capacitive currents upon short stimulus application offers a sensitive and efficient way to screen for sensory ligands (*e.g.,* major urinary proteins; MUPs) that activate defined populations of cells[51] (**Figure 5B**).

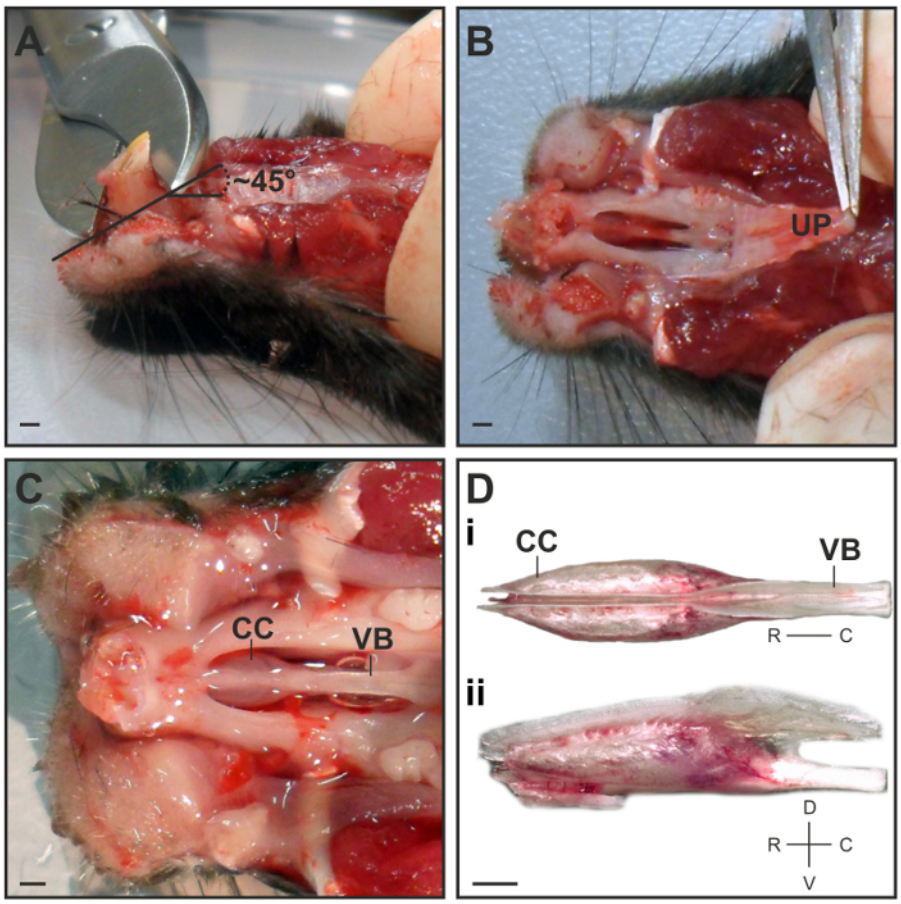

Figure 1: Dissection of the VNO. (**A**) Side view on the mouse head to illustrate the position and angle at which the incisors are cut. (**B**) Ventral view depicting the best point to grab and peel back the upper palate (UP). (**C**) Ventral view onto the cartilage capsule (CC) that harbors the VNO and the vomer bone (VB) after removing the lower jaw, incisors and palate. (**D**) Dorsal view of the dissected VNO capsule depicting the bilateral localization of both VNOs (D_i). The lateral view illustrates the rim of cartilage on the dorsal side where both VNOs need to be separated (D_{ii}). Scale bar = 1 mm (**A**-**D**). Please click here to view a larger version of this figure.

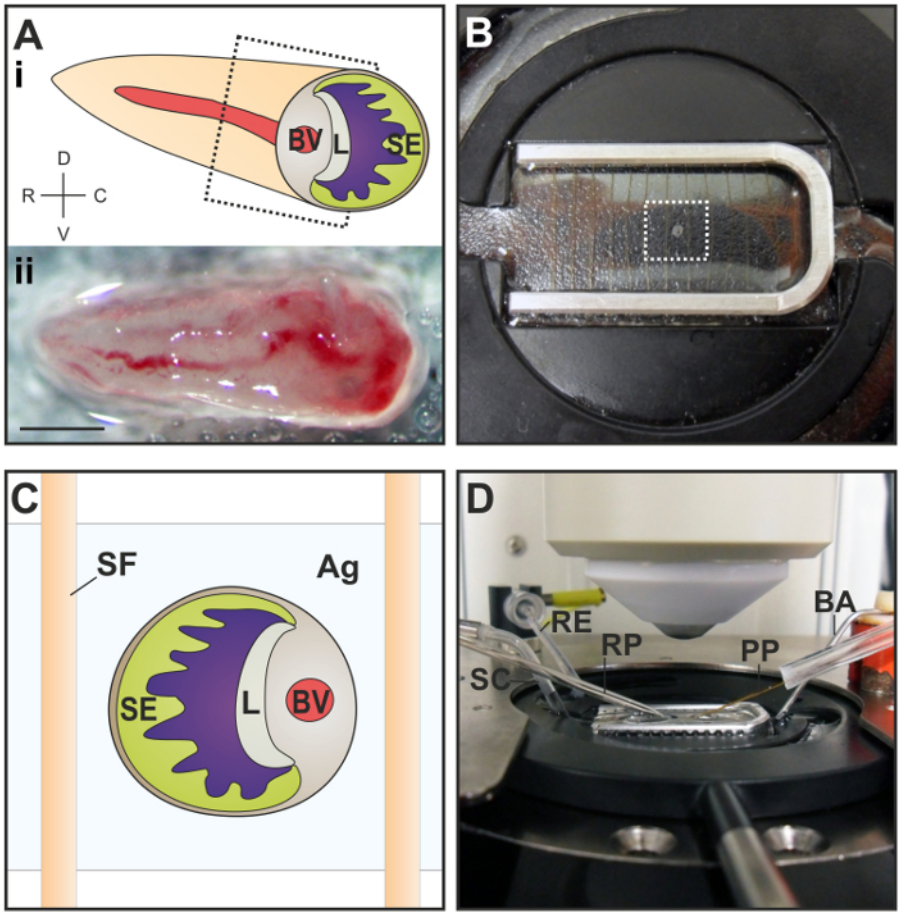

Figure 2: Tissue preparation, recording chamber and microscope stage. Schematic lateral view on a VNO to illustrate the course and position of the large blood vessel (BV) in the non-sensory part of the epithelium (**A**$_i$). The dashed line represents the coronal slicing layer. Lateral view on a VNO peeled out of the CC shows the blood vessel (**A**$_{ii}$). (**B**) Agarose-embedded coronal VNO tissue slice fixed to the bottom of the solution-filled recording chamber using a stainless steel anchor wired with 0.1 mm thick synthetic fiber (SF) threads. The boxed area depicts the agarose surrounding the tissue slice. (**C**) Schematic view illustrating the position and orientation of an agarose (Ag)-embedded coronal VNO slice positioned between two fibers. (**D**) Overview of the recording chamber placed on the microscope stage. The chamber is equipped with bath application (BA) for constant superfusion with oxygenated S_2, the perfusion pencil (PP) to apply sensory stimuli or pharmacological agents, the recording pipette (RP) connected to the amplifier head stage, the reference electrode (RE) and the suction capillary (SC) to maintain a constant exchange of solution in the chamber. Scale bar = 1 mm (**A**$_{ii}$). Please click here to view a larger version of this figure.

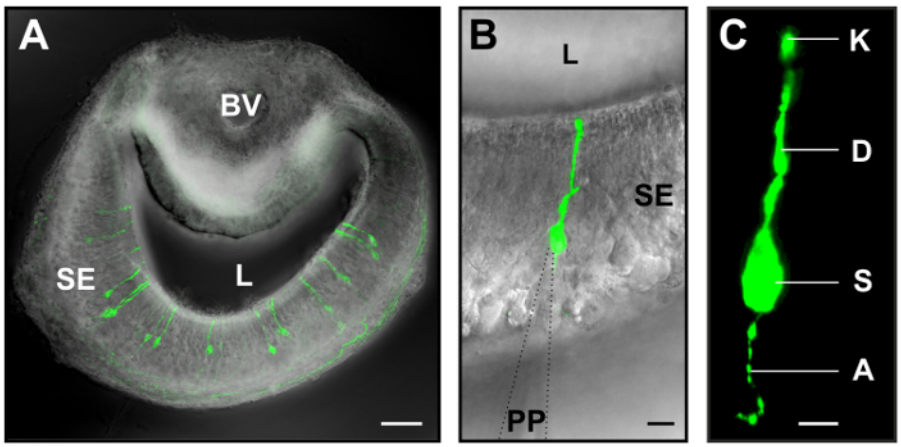

Figure 3: Coronal VNO tissue slice. (**A**) Confocal image (maximum projection) of a 150 µm acute coronal VNO tissue slice showing the distribution of fluorescent FPR-rs3 tau-Venus$^+$ neurons (green) in the vomeronasal sensory epithelium. Blood vessel (BV), lumen (L), sensory epithelium (SE). (**B**) FPR-rs3 tau-Venus$^+$ neurons exhibit a single apical dendrite ending in a knob-like structure at the luminal border. Whole-cell patch-clamp recordings were performed from the VSN soma, patch pipette (PP). (**C**) Morphology of a single VSN with the dendritic knob (K) at the tip of the long and narrow dendrite (D), the cell soma (S) and the axon (A) leaving the soma at the basal side. Scale bars, 50 µm (**A**), 10 µm (**B**), 5 µm (**C**). This figure has been modified from[52]. Please click here to view a larger version of this figure.

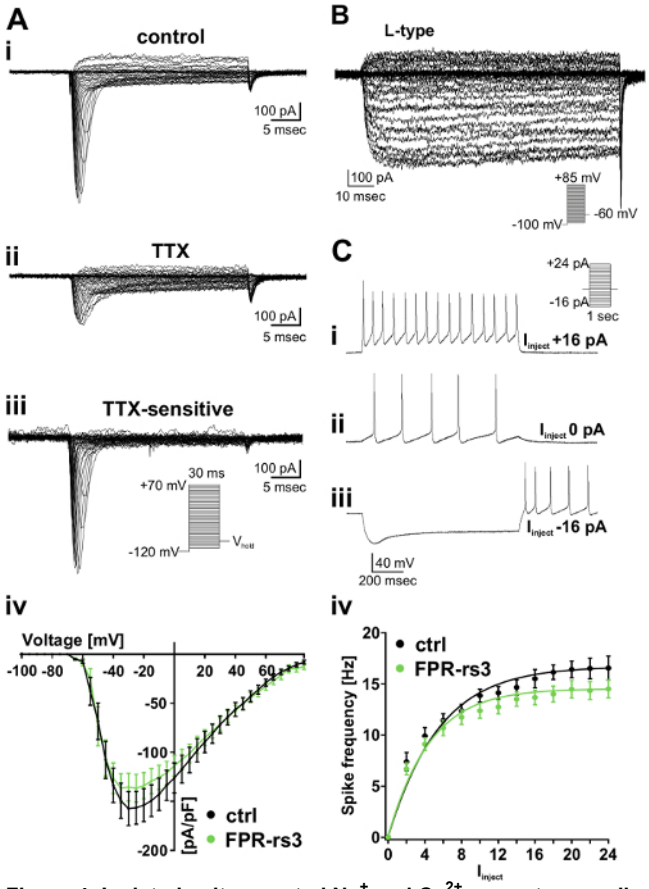

Figure 4: Isolated voltage-gated Na^+ and Ca^{2+} currents as well as spike discharge. (**A**) Representative traces from whole-cell patch-clamp recordings of a TTX-sensitive fast activating Na^+ current in FPR-rs3$^+$ VSNs. (**A_i**) Voltage step recording under control conditions (extracellular solution S_1; intracellular solution S_4) reveals a voltage-dependent fast and transient inward current. (**A_{ii}**) TTX treatment (1 µM) strongly diminishes the current. Digitally subtracted trace (control-TTX (**A_{iii}**)) reveals the TTX-sensitive voltage-gated Na^+ current. Current-voltage relationships of TTX-sensitive Na^+ currents isolated from control and FPR-rs3$^+$ neurons (**A_{iv}**). (**B**) Representative Ca^{2+} current traces isolated pharmacologically (10 µM nifedipine). (**C**) Representative current clamp traces showing de- /hyperpolarization and trains of (rebound) action potentials generated upon stepwise positive (**C_i**) and negative (**C_{iii}**) current injection. Note the spontaneous activity measured at 0 pA current injection (**C_{ii}**). (**C_{iv}**) Firing frequency of control and FPR-rs3$^+$ neurons as a function of the injected current (I_{inject}). The gradual increase in firing rate is similar for control and FPR-rs3$^+$ VSNs. Note that VSNs are exquisitely sensitive to current injections even in the low picoamperes range[53-56]. Note that *f*-I curves have been "background-corrected" using the spontaneous spiking frequency at 0 pA current injection. Data are means ± SEM. This figure has been modified from[52]. Please click here to view a larger version of this figure.

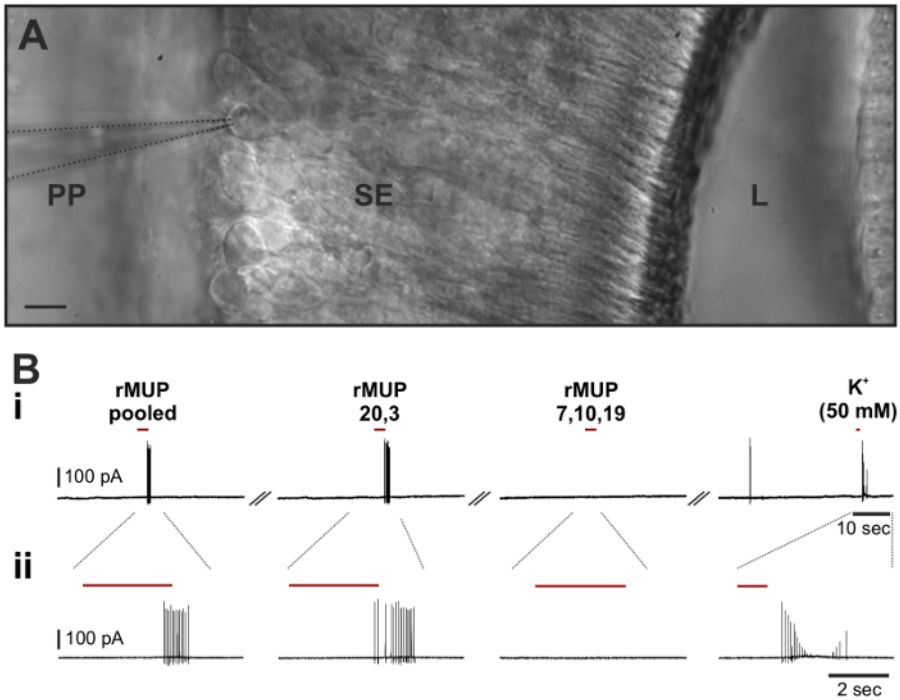

Figure 5: Extracellular 'loose patch' recordings from basal VSNs. (**A**) IR-DIC image of an acute VNO tissue slice depicting the recording pipette in the basal layer of the sensory epithelium. (**B**) Representative original recording of a basal VSN in the cell-attached configuration ('loose-seal') responding with short transient bursts of spikes to brief stimulations (3 sec) with pooled recombinantly expressed major urinary proteins (rMUPs) and an elevated potassium concentration (50 mM, 1 sec), respectively ($\mathbf{B_i}$). Higher magnification of recordings shown in ($\mathbf{B_i}$) illustrates bursts of spikes in response to stimulations ($\mathbf{B_{ii}}$). Red bars indicate time of stimulation, inter-stimulus interval = 30 sec, continuous recording, interruptions <1 sec (cut marks //). Scale bar = 5 µm (**A**). Panel (**A**) has been modified from reference[38]. Please click here to view a larger version of this figure.

Discussion

The VNO is a chemosensory structure that detects semiochemicals. To date, the majority of vomeronasal receptors remains to be deorphanized as only few receptor-ligand pairs have been identified. Among those, V1rb2 was described to be specifically activated by the male urinary pheromone 2-heptanone[30], V2rp5 to be activated by the male specific pheromone ESP1[57] as well as V2r1b and V2rf2 to be activated by the MHC peptides SYFPEITHI[48] and SEIDLILGY[58], respectively. A prerequisite to understanding receptor-ligand relationships and signal transduction is knowledge of the biophysical characteristics of defined VSN populations in a native environment. Passive and active membrane properties, voltage-gated ionic conductances and action potential discharge patterns define the means and extent to which receptor neurons respond to chemosensory stimuli. Electrophysiological recordings in acute tissue slices and, in particular, whole-cell patch-clamp recordings provide an excellent method to analyze these properties in great detail.

A critical step for successful and reliable physiological recordings in tissue slices is the preparation itself. To maximize the time span to perform experiments, the tissue must be sliced and transferred to ice-cold oxygenated solution immediately after dissection. Following that, slices can be kept for several hr allowing analysis of a substantial number of cells per experimental day. It takes some practice to reduce time to dissect and embed both VNOs of one animal in less than 30 min. After that, the success rate for an experienced experimenter to obtain several intact tissue slices with viable cells is well above 75%. Performing patch-clamp recordings is a low-throughput experimental approach in comparison to Ca^{2+} imaging. Yet, it allows a more detailed and versatile analysis of activity on the single-cell level with a much higher temporal resolution. In the whole-cell configuration, the intracellular medium is dialyzed by the pipette solution. While the pipette solution might not reflect the exact cytosolic composition, it provides the experimenter with exact control over both extra- and intracellular ionic conditions. For reliable interpretation of results, continuous monitoring of access resistance and leak current is crucial. At times, a significant increase or strong change in access resistance or leak current leads to uninterpretable results and thus demands these recordings to be discarded. Moreover, it is important to note that some pharmacological compounds bind irreversibly rendering it necessary to replace slices after each recording.

Recording in the cell-attached configuration prevents dialysis of intracellular components and does not influence the cell's membrane potential. Thus, this technique provides a less invasive and relatively fast way of screening. However, this approach is generally limited to the recording of super-threshold action potential-driven capacitive currents from the outside of the cell membrane. Loose-patch recordings have proven to be suitable for analyzing the spiking behavior of larger numbers of sensory neurons in VNO slices[38,54].

The transgenic model employed here provides a reliable tool to identify and analyze the population of FPR-rs3 expressing VSNs. Moreover, the technique described here can be extended to other lines regardless of their genotype. Despite the enormous advantage of investigating a defined cell type, using transgenic mice limits experiments to the available lines. Recently, however, targeted genome editing has become faster and more affordable with the CRISPR/Cas9 technique[59]. In conclusion, targeted patch-clamp recordings in acute vomeronasal tissue slices provide a versatile approach to characterize biophysical and physiological properties of a defined population of sensory neurons.

Disclosures

The authors have nothing to disclose.

Acknowledgements

We thank Ivan Rodriguez and Benoit von der Weid for generating the FPR-rs3-i-venus mouse line, their constructive criticism and fruitful discussions. This work was funded by grants of the Volkswagen Foundation (I/83533), the Deutsche Forschungsgemeinschaft (SP724/6-1) and by the Excellence Initiative of the German federal and state governments. MS is a Lichtenberg Professor of the Volkswagen Foundation.

References

1. Firestein, S. How the olfactory system makes sense of scents. *Nature.* **413** (6852), 211-8 (2001).
2. Mombaerts, P. Genes and ligands for odorant, vomeronasal and taste receptors. *Nat. Rev. Neurosci.* **5** (4), 263-78 (2004).
3. Fuss, S. H., Omura, M., & Mombaerts, P. The Grueneberg ganglion of the mouse projects axons to glomeruli in the olfactory bulb. *Eur. J. Neurosci.* **22** (10), 2649-54 (2005).
4. Roppolo, D., Ribaud, V., Jungo, V. P., Lüscher, C., & Rodriguez, I. Projection of the Grüneberg ganglion to the mouse olfactory bulb. *Eur. J. Neurosci.* **23** (11), 2887-94 (2006).
5. Adams, D. R. Fine structure of the vomeronasal and septal olfactory epithelia and of glandular structures. *Microsc. Res. Tech.* **23** (1), 86-97 (1992).
6. Ma, M., *et al.* Olfactory signal transduction in the mouse septal organ. *J. Neurosci.* **23** (1), 317-24 (2003).
7. Dulac, C., & Torello, A. T. Molecular detection of pheromone signals in mammals: from genes to behaviour. *Nat. Rev. Neurosci.* **4** (7), 551-62 (2003).
8. Luo, M., & Katz, L. C. Encoding pheromonal signals in the mammalian vomeronasal system. *Curr. Opin. Neurobiol.* **14** (4), 428-34 (2004).
9. Brennan, P. A., & Kendrick, K. M. Mammalian social odours: attraction and individual recognition. *Philos. Trans. R. Soc. Lond. B. Biol. Sci.* **361** (1476), 2061-78 (2006).
10. Tirindelli, R., Dibattista, M., Pifferi, S., & Menini, A. From Pheromones to Behavior. *Physiol. Rev.* **89**, 921-956 (2009).
11. Jacobson, L., Trotier, D., & Doving, K. B. Anatomical description of a new organ in the nose of domesticated animals by Ludvig Jacobson (1813). *Chem. Senses.* **23** (6), 743-54 (1998).
12. Keverne, E. B. The Vomeronasal Organ. *Science.* **286** (5440), 716-720 (1999).
13. Breer, H., Fleischer, J., & Strotmann, J. The sense of smell: multiple olfactory subsystems. *Cell. Mol. Life Sci. C.* **63** (13), 1465-75 (2006).
14. Liberles, S. D. Mammalian pheromones. *Annu. Rev. Physiol.* **76**, 151-75 (2014).
15. Meredith, M., & O'Connell, R. J. Efferent control of stimulus access to the hamster vomeronasal organ. *J. Physiol.* **286**, 301-16 (1979).
16. Pankevich, D., Baum, M. J., & Cherry, J. A. Removal of the superior cervical ganglia fails to block Fos induction in the accessory olfactory system of male mice after exposure to female odors. *Neurosci. Lett.* **345** (1), 13-6 (2003).
17. Giacobini, P., Benedetto, A., Tirindelli, R., & Fasolo, A. Proliferation and migration of receptor neurons in the vomeronasal organ of the adult mouse. *Brain Res. Dev. Brain Res.* **123** (1), 33-40 (2000).
18. Coppola, D. M., & O'Connell, R. J. Stimulus access to olfactory and vomeronasal receptors in utero. *Neurosci. Lett.* **106** (3), 241-8 (1989).
19. Hovis, K. R., *et al.* Activity Regulates Functional Connectivity from the Vomeronasal Organ to the Accessory Olfactory Bulb. *J. Neurosci.* **32** (23), 7907-7916 (2012).
20. Mucignat-Caretta, C. The rodent accessory olfactory system. *J. Comp. Physiol. A Neuroethol. Sensory, Neural, Behav. Physiol.* **196** (10), 767-777 (2010).
21. Jia, C., & Halpern, M. Subclasses of vomeronasal receptor neurons: differential expression of G proteins (Giα2 and G(αo)) and segregated projections to the accessory olfactory bulb. *Brain Res.* **719** (1-2), 117-28 (1996).
22. Del Punta, K., Puche, A. C., Adams, N. C., Rodriguez, I., & Mombaerts, P. A divergent pattern of sensory axonal projections is rendered convergent by second-order neurons in the accessory olfactory bulb. *Neuron.* **35** (6), 1057-66 (2002).
23. Belluscio, L., Koentges, G., Axel, R., & Dulac, C. A map of pheromone receptor activation in the mammalian brain. *Cell.* **97** (2), 209-220 (1999).
24. Rodriguez, I., Feinstein, P., & Mombaerts, P. Variable patterns of axonal projections of sensory neurons in the mouse vomeronasal system. *Cell.* **97** (2), 199-208 (1999).
25. Rivière, S., Challet, L., Fluegge, D., Spehr, M., & Rodriguez, I. Formyl peptide receptor-like proteins are a novel family of vomeronasal chemosensors. *Nature.* **459** (7246), 574-7 (2009).
26. Martini, S., Silvotti, L., Shirazi, A., Ryba, N. J. P., & Tirindelli, R. Co-expression of putative pheromone receptors in the sensory neurons of the vomeronasal organ. *J. Neurosci.* **21** (3), 843-8 (2001).
27. Matsuoka, M., *et al.* Immunocytochemical study of Gi2alpha and Goalpha on the epithelium surface of the rat vomeronasal organ. *Chem. Senses* **26** (2), 161-6 (2001).
28. Dulac, C., & Torello, A. T. Molecular detection of pheromone signals in mammals: from genes to behaviour. *Nat. Rev. Neurosci.* **4** (7), 551-62 (2003).
29. Leinders-Zufall, T., *et al.* Ultrasensitive pheromone detection by mammalian vomeronasal neurons. *Nature* **405** (6788), 792-6 (2000).
30. Boschat, C., *et al.* Pheromone detection mediated by a V1r vomeronasal receptor. *Nat. Neurosci.* **5** (12), 1261-2 (2002).
31. Novotny, M. V. Pheromones, binding proteins and receptor responses in rodents. *Biochem. Soc. Trans.* **31**, 117-22 (2003).
32. Nodari, F., *et al.* Sulfated steroids as natural ligands of mouse pheromone-sensing neurons. *J. Neurosci.* **28** (25), 6407-18 (2008).
33. Isogai, Y., *et al.* Molecular organization of vomeronasal chemoreception. *Nature* **478** (7368), 241-5 (2011).
34. Leinders-Zufall, T., *et al.* MHC class I peptides as chemosensory signals in the vomeronasal organ. *Science* **306** (5698), 1033-7 (2004).
35. Chamero, P., *et al.* Identification of protein pheromones that promote aggressive behaviour. *Nature* **450** (7171), 899-902 (2007).

36. Kimoto, H., Haga, S., Sato, K., & Touhara, K. Sex-specific peptides from exocrine glands stimulate mouse vomeronasal sensory neurons. *Nature.* **437** (7060), 898-901 (2005).
37. Ferrero, D. M., *et al.* A juvenile mouse pheromone inhibits sexual behaviour through the vomeronasal system. *Nature* **502** (7471), 368-71 (2013).
38. Kaur, A. W., *et al.* Murine pheromone proteins constitute a context-dependent combinatorial code governing multiple social behaviors. *Cell* **157** (3), 676-88 (2014).
39. Ben-Shaul, Y., Katz, L. C., Mooney, R., & Dulac, C. In vivo vomeronasal stimulation reveals sensory encoding of conspecific and allospecific cues by the mouse accessory olfactory bulb. *PNAS.* **107** (11), 5172-7 (2010).
40. Kimoto, H., *et al.* Sex- and strain-specific expression and vomeronasal activity of mouse ESP family peptides. *Curr. Biol.* **17** (21), 1879-84 (2007).
41. Spehr, M., *et al.* Parallel processing of social signals by the mammalian main and accessory olfactory systems. *Cell. Mol. Life Sci. C.* **63** (13), 1476-84 (2006).
42. Chamero, P., *et al.* G protein G{alpha}o is essential for vomeronasal function and aggressive behavior in mice. *PNAS* (2011).
43. Bufe, B., Schumann, T., & Zufall, F. Formyl peptide receptors from immune and vomeronasal system exhibit distinct agonist properties. *J. Biol. Chem.* **287** (40), 33644-55 (2012).
44. Bozza, T., Feinstein, P., Zheng, C., & Mombaerts, P. Odorant receptor expression defines functional units in the mouse olfactory system. *J. Neurosci.* **22** (8), 3033-43 (2002).
45. Grosmaitre, X., Vassalli, A., Mombaerts, P., Shepherd, G. M., & Ma, M. Odorant responses of olfactory sensory neurons expressing the odorant receptor MOR23: a patch clamp analysis in gene-targeted mice. *PNAS.* **103** (6), 1970-5 (2006).
46. Oka, Y., *et al.* Odorant receptor map in the mouse olfactory bulb: in vivo sensitivity and specificity of receptor-defined glomeruli. *Neuron.* **52** (5), 857-69 (2006).
47. Ukhanov, K., Leinders-Zufall, T., & Zufall, F. Patch-clamp analysis of gene-targeted vomeronasal neurons expressing a defined V1r or V2r receptor: ionic mechanisms underlying persistent firing. *J. Neurophysiol.* **98** (4), 2357-69 (2007).
48. Leinders-Zufall, T., Ishii, T., Mombaerts, P., Zufall, F., & Boehm, T. Structural requirements for the activation of vomeronasal sensory neurons by MHC peptides. *Nat. Neurosci.* **12** (12), 1551-8 (2009).
49. Pacifico, R., Dewan, A., Cawley, D., Guo, C., & Bozza, T. An olfactory subsystem that mediates high-sensitivity detection of volatile amines. *Cell Rep.* **2** (1), 76-88 (2012).
50. Veitinger, S., *et al.* Purinergic signalling mobilizes mitochondrial Ca^{2+} in mouse Sertoli cells. *J. Physiol.* **589** (Pt 21), 5033-55 (2011).
51. Kaur, A. W., *et al.* Murine pheromone proteins constitute a context-dependent combinatorial code governing multiple social behaviors. *Cell.* **157** (3), 676-88 (2014).
52. Ackels, T., von der Weid, B., Rodriguez, I., & Spehr, M. Physiological characterization of formyl peptide receptor expressing cells in the mouse vomeronasal organ. *Front. Neuroanat.* **8** (November), 1-13 (2014).
53. Liman, E. R., & Corey, D. P. Electrophysiological characterization of chemosensory neurons from the mouse vomeronasal organ. *J. Neurosci.* **16** (15), 4625-37 (1996).
54. Cichy, A., *et al.* Extracellular pH Regulates Excitability of Vomeronasal Sensory Neurons. *J. Neurosci.* **35** (9), 4025-4039 (2015).
55. Shimazaki, R., *et al.* Electrophysiological properties and modeling of murine vomeronasal sensory neurons in acute slice preparations. *Chem. Senses.* **31** (5), 425-35 (2006).
56. Hagendorf, S., Fluegge, D., Engelhardt, C., & Spehr, M. Homeostatic control of sensory output in basal vomeronasal neurons: activity-dependent expression of ether-à-go-go-related gene potassium channels. *J. Neurosci.* **29** (1), 206-21 (2009).
57. Haga, S., *et al.* The male mouse pheromone ESP1 enhances female sexual receptive behaviour through a specific vomeronasal receptor. *Nature.* **466** (7302), 118-22 (2010).
58. Leinders-Zufall, T., *et al.* A family of nonclassical class I MHC genes contributes to ultrasensitive chemodetection by mouse vomeronasal sensory neurons. *J. Neurosci.* **34** (15), 5121-33 (2014).
59. Jinek, M., *et al.* A programmable dual-RNA-guided DNA endonuclease in adaptive bacterial immunity. *Science.* **337** (August), 816-821 (2012).

